

Reduction of fumarate, mesaconate and crotonate by Mfr, a novel oxygen-regulated periplasmic reductase in *Campylobacter jejuni*

Edward Guccione,^{1†} Andrew Hitchcock,^{1†}
Stephen J. Hall,^{1†} Francis Mulholland,² Neil Shearer,²
Arnoud H. M. van Vliet² and David J. Kelly^{1*}

¹Department of Molecular Biology and Biotechnology,
The University of Sheffield, Firth Court, Western Bank,
Sheffield S10 2TN, UK.

²Institute of Food Research, Norwich Research Park,
Colney Lane, Norwich NR4 7UA, UK.

Summary

Methylmenaquinol : fumarate reductase (Mfr) is a newly recognized type of fumarate reductase present in some ϵ -proteobacteria, where the active site subunit (MfrA) is localized in the periplasm, but for which a physiological role has not been identified. We show that the *Campylobacter jejuni mfrABE* operon is transcribed from a single promoter, with the *mfrA* gene preceded by a small open reading-frame (*mfrX*) encoding a *C. jejuni*-specific polypeptide of unknown function. The growth characteristics and enzyme activities of mutants in the *mfrA* and menaquinol : fumarate reductase A (*frdA*) genes show that the cytoplasmic facing Frd enzyme is the major fumarate reductase under oxygen limitation. The Mfr enzyme is shown to be necessary for maximal rates of growth by fumarate respiration and rates of fumarate reduction in intact cells measured by both viologen assays and ¹H-NMR were slower in an *mfrA* mutant. As periplasmic fumarate reduction does not require fumarate/succinate antiport, Mfr may allow more efficient adaptation to fumarate-dependent growth. However, a further rationale for the periplasmic location of Mfr is suggested by the observation that the enzyme also reduces the fumarate analogues mesaconate and crotonate; fermentation products of anaerobes with which *C. jejuni* shares its gut environment, that are unable to be transported into the cell. Both MfrA and

MfrB subunits were localized in the periplasm by immunoblotting and 2D-gel electrophoresis, but an *mfrE* mutant accumulated unprocessed MfrA in the cytoplasm, suggesting a preassembled MfrABE holoenzyme has to be recognized by the TAT system for translocation to occur. Gene expression studies in chemostat cultures following an aerobic-anaerobic shift showed that *mfrA* is highly upregulated by oxygen limitation, as would be experienced *in vivo*. Our results indicate that in addition to a role in fumarate respiration, Mfr allows *C. jejuni* to reduce analogous substrates specifically present in the host gut environment.

Introduction

Campylobacter jejuni is a human pathogen of major public health and environmental significance. It is the leading cause of acute bacterial gastroenteritis worldwide and is acquired predominantly by ingesting contaminated food, milk or water (Jacobs-Reitsma *et al.*, 2008). As a common commensal of the gastrointestinal tract of many bird species, poultry serves as the primary source of human infection (Wagenaar *et al.*, 2008). *Campylobacter jejuni* also has the ability to survive in a variety of environmental niches outside of the host, but the factors contributing to its adaptability are poorly understood, particularly since it is an oxygen-sensitive microaerophile with a small genome. Significantly, *C. jejuni* has a surprisingly complex branched electron transport chain (Kelly, 2008), which includes a number of terminal reductases allowing energy conservation with alternative electron acceptors present in various environments, such as nitrate, nitrite, hydrogen peroxide, trimethylamine-N-oxide, dimethylsulfoxide and fumarate (Sellars *et al.*, 2002; Pittman *et al.*, 2007; Weingarten *et al.*, 2008; 2009).

Fumarate reduction is carried out by succinate : quinone oxidoreductases (SQORs), which are membrane-bound multisubunit complexes that catalyse the two-electron transfer between the succinate/fumarate and quinone/quinol redox couples. Those which perform succinate oxidation are defined as succinate : quinone reductases (SQRs), commonly referred to as 'succinate dehydrogenases', and those which perform fumarate

Received 17 August, 2009; accepted 23 September, 2009. *For correspondence. E-mail d.kelly@sheffield.ac.uk; Tel. (+44) 114 222 4414; Fax (+44) 114 272 8697. †Present address: Manchester Interdisciplinary Biocentre, University of Manchester, 131 Princess Street, Manchester M1 7DN, UK. ‡These authors contributed equally to this work.

reduction are termed quinol:fumarate reductases (QFR) or 'fumarate reductases'. It is difficult, however, on the basis of sequence analysis alone, to predict whether a given enzyme will function as an SQR or a QFR *in vivo* (Lancaster, 2002). Succinate : quinone reductases are key citric-acid cycle enzymes under aerobic conditions, and QFRs operate in anaerobic respiration with fumarate as the terminal electron acceptor. Both are comprised of a soluble domain attached to or associated with the cytoplasmic membrane through one or two polypeptides. The soluble domain is comprised of two subunits; subunit A contains an FAD cofactor and is the site of fumarate reduction and succinate oxidation, and subunit B contains three iron-sulfur centres (Lancaster, 2002; Lemos *et al.*, 2002). The membrane-associated domain consists of two hydrophobic subunits (C and D) or a single fusion protein, and may contain one or two haems, which conduct electrons from/to the quinone pool.

Succinate : quinone oxidoreductases are currently classified as types A–E (Lancaster, 2002; Lemos *et al.*, 2002), based on mechanism, the type of membrane-bound domain and number of haems present. Type A SQOR enzymes are found in many archaea and contain two hydrophobic subunits, each with two haem groups. Type B enzymes contain a single large hydrophobic subunit with two haem groups. The QFRs of the related ϵ -proteobacteria, *C. jejuni*, *Helicobacter pylori* and *Wolinella succinogenes* are of this type (Lancaster and Simon, 2002; Mileni *et al.*, 2006), as is the SQR of *Bacillus subtilis*. However, while the known B type enzymes have an overall similar structure, they show significant branching phylogenetically and may function with distinct mechanisms (Lemos *et al.*, 2002; Lancaster *et al.*, 2005; Zaubmüller *et al.*, 2006). Type C and D enzymes possess two hydrophobic subunits with one or no haem group respectively.

E-type SQORs were recently discovered in the *Sulfolobales* order of the archaea, including some species in the genera *Acidianus* (Lemos *et al.*, 2001) and *Sulfolobus* (Janssen *et al.*, 1997), and characterized as unidirectional SQRs (Lemos *et al.*, 2002). They are structurally very different from all other SQOR classes. First, instead of the 3Fe-4S cluster found in the B subunit of all other types of SQOR, E type enzymes contain an additional 4Fe-4S cluster. Second, the membrane-associated domain of E type SQORs (one or two subunits, SdhE and SdhF) is weakly hydrophobic, does not span the membrane and is unrelated in sequence to the SdhC/D subunits of other SQORs (Lemos *et al.*, 2002). A further unusual feature is the presence of a cysteine-rich motif within SdhE, which is thought to have redox activity with quinone (Lemos *et al.*, 2002). The function of the smaller SdhF subunit is unknown. Among bacteria, E-type SQORs are rare but some ϵ -proteobacteria including

C. jejuni and *W. succinogenes* possess enzymes annotated as succinate dehydrogenases that have a similar subunit organization and some sequence similarities to the archaeal E-type SQRs. The latter enzymes donate electrons to the electropositive caldariella quinone ($E_{m,7}$ +103 mV) and thus the reduction of this quinone by the oxidation of succinate to fumarate ($E_{m,7}$ +30 mV) is exergonic. However, the presence of an E-type SQR in bacteria like *C. jejuni* and *W. succinogenes* would pose a bioenergetic problem, as the reduction of the electronegative menaquinone (MK, $E_{m,7}$ -75 mV) by succinate will be endergonic and requires coupling to the proton-motive force (Zaubmüller *et al.*, 2006), but this cannot occur in the absence of a membrane-spanning haem-containing subunit. This paradox was solved recently when the E-type 'succinate dehydrogenase' from *W. succinogenes* was homologously overexpressed and identified as a novel type of methylmenaquinol : fumarate reductase (Mfr), in which the active site is located in the periplasm by virtue of a twin-arginine translocation (TAT) signal peptide sequence at the N-terminus of the flavoprotein subunit (Juhnke *et al.*, 2009). The enzyme does not oxidize succinate and preferentially uses methylmenaquinol (mMKH₂, $E_{m,7}$ -124 mV) rather than menaquinol (MKH₂) in fumarate reduction. Furthermore, the FAD cofactor in the enzyme is non-covalently bound. However, the activity of this enzyme in cell extracts of wild-type *W. succinogenes* could not be detected in the study of Juhnke and colleagues (2009), and its physiological role is unknown.

Campylobacter jejuni also contains mMKH₂, in equimolar amounts with MKH₂ (Carlone and Anet, 1986) and its Mfr subunits are homologous to those of *W. succinogenes*. Here, we show that Mfr-dependent fumarate reductase activity can be detected in periplasmic fractions of wild-type *C. jejuni* cells and we have constructed single and double mutants in the *frdA* and *mfrA* genes, which has allowed an assessment to be made of the physiological role of each enzyme. Mfr makes a contribution to fumarate-dependent growth under oxygen-limited conditions, but the enzyme was also found to reduce mesaconate and crotonate, substrates potentially present in the gut environment but which do not appear to be transported into the cell, thus providing a rationale for the periplasmic location of Mfr. The characterization of the *mfr* genes of *C. jejuni* revealed the presence of an additional gene of unknown function, *mfrX*, upstream of *mfrA*. The expression of the *mfrA* gene was found to be highly upregulated under oxygen limitation. In addition to *C. jejuni* and *W. succinogenes*, an MfrABE-like complex is encoded in the genomes of only a few other animal commensals and pathogens (*C. concisus*, *C. curvus* and the unrelated gut bacterium *Mitsuokella multacida*), indicating a specialized role in the host.

Results

Structure and transcriptional analysis of the *mfr* operon of *C. jejuni* and distribution of similar enzymes in other bacteria

The *cj0437–0439* genes encode the annotated succinate dehydrogenase of *C. jejuni* NCTC 11168, consisting of the active site containing flavoprotein (Cj0437), iron–sulfur subunit (Cj0438) and cysteine rich SdhE homologue (Cj0439), characteristic of an E-type SQOR. There is no gene encoding an SdhF homologue. We initially tried to determine the transcription start site of the *cj0437–0439* operon using 5' RACE with a primer located in the *cj0437* gene, but were unable to obtain a specific product (Fig. 1B, lanes 3 and 4), suggesting that the transcription start site was further upstream. Examination of the 5' untranslated region upstream of *cj0437* revealed a good ribosome binding site preceding a small open reading frame (ORF) not annotated in any *C. jejuni* genome sequences, with the potential to encode a 60-residue protein of predicted pI of 8.88 and a molecular weight of 7577 Da (see Fig. 1A and C). The deduced product, tentatively named MfrX, is not homologous to SdhF or any other protein in the GenBank/EMBL databases. It contains three cysteine residues and a single predicted transmembrane helix. A mutant was constructed in the *mfrX* ORF, but this showed no difference in growth compared

with the wild-type under either microaerobic or oxygen-limited growth conditions. This mutant still produced MfrA as shown by immunoblotting with an MfrA-specific antibody (data not shown). Using a primer located in the upstream sequences we were able to map a single, specific transcription start site 242 nt upstream of the *cj0437* start codon (Fig. 1A), and 23 nt upstream of the predicted *mfrX* start codon (Fig. 1A). Cloning of the non-specific cDNA PCR product obtained when using the primer located in *cj0437* showed that this fragment starts 109 nt upstream of the *mfrA* start codon, indicating that the *mfrX-mfrABE* mRNA is post-transcriptionally processed towards higher stability of a transcript containing only the *mfrABE* genes (Fig. 1A and B). This post-transcriptional processing was also noticed in a high-throughput sequencing survey of the complete set of transcribed sequences of *C. jejuni* (I. Porcelli, C.M. Sharma, M. Reuter, J. Vogel and A.H.M. van Vliet, unpubl. data).

Like the *W. succinogenes* MfrA protein, the Cj0437 subunit possesses an N-terminal Twin Arginine Translocase (TAT) consensus sequence (SRRDFIK) within a signal peptide region, which scores as a correct match using the TatP 1.0 web server. BLAST searching of the genome sequence databases for SdhA homologues that also contain a TAT-like signal peptide revealed that, in addition to *W. succinogenes* and other sequenced strains of *C. jejuni*, the oral campylobacters *C. concisus*

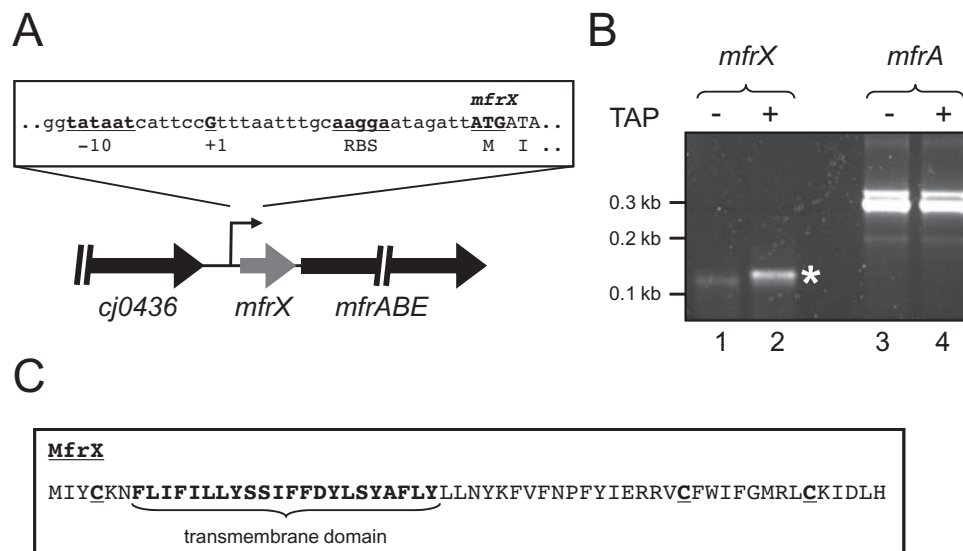


Fig. 1. The *mfrABE* genes are cotranscribed with a small open reading frame tentatively named *mfrX*, and the *mfr(X)ABE* mRNA is likely to be post-transcriptionally modified.

A. Schematic representation of the *mfr(X)ABE* promoter region. The promoter region including the -10 sequence, transcriptional start site (+1), ribosome binding site (RBS) and translation initiation codon are shown.

B. 5' RACE determination of the *mfr(X)ABE* transcript start site. Lanes 1 and 2 are 5' RACE with a primer located in *mfrX*, lanes 3 and 4 with a primer located in *mfrA*. Addition of tobacco acid phosphatase (TAP) is indicated above the lanes. The asterisk indicates a TAP-specific cDNA product, corresponding with the transcription start site shown in Fig. 1A. The high level of product in lanes 3 and 4 is suggestive of post-transcriptional modification of the *mfr(X)ABE* mRNA to one containing only *mfrABE*, starting at residue 405224 in the *C. jejuni* NCTC 11168 genome sequence (Parkhill *et al.*, 2000; Gundogdu *et al.*, 2007). Relevant marker sizes are shown on the left.

C. Features of the predicted MfrX protein sequence. Cysteines are underlined, the putative transmembrane domain is indicated.

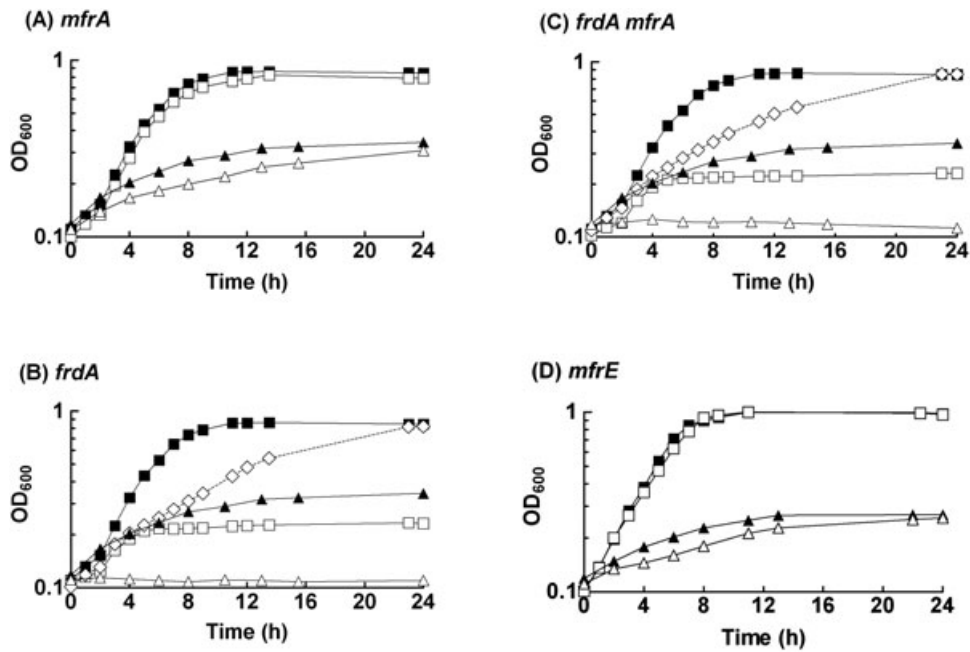


Fig. 2. Microaerobic growth (squares) or oxygen-limited growth (triangles) of wild-type (closed symbols) and mutants (open symbols) in BHI-FCS media. For microaerobic growth, un-supplemented BHI-FCS was used, except where the dashed line with open diamonds shows the effect of 20 mM sodium fumarate on microaerobic growth of the mutant strains indicated (B and C). For oxygen limited growth BHI-FCS supplemented with 40 mM sodium fumarate was used. In the absence of fumarate, none of the strains was able to grow under oxygen limitation (data not shown). All data are representative of at least two independent growth experiments.

and *C. curvus* also encode a similar enzyme. *C. doylei* encodes *mfrXABE* homologues but only as pseudogenes. Other than these ϵ -proteobacteria, only the human gut bacterium *Mitsuokella multacida* was found to possess an obvious TAT signal peptide containing SdhA-like subunit. In each of these cases an SdhE homologue (MfrE) is also encoded in the same operon.

Mutation of frdA, but not mfrA, causes a severe aerobic and oxygen-limited growth defect

In order to study the role of the *mfr* gene products in comparison to the type B fumarate reductase encoded by the *frdCAB* operon in *C. jejuni*, single and double mutants were created in the genes encoding the FAD and substrate binding A-subunit of both complexes, *frdA* (*cj0409*) and *mfrA* (*cj0437*). The *frd* operon is transcribed from the same strand as the downstream gene, *cj0411* (encoding a putative ATP/GTP binding protein). Although we were unable to obtain any *C. jejuni* transformants using a *frdA* complementation plasmid, RT-PCR showed a small increase in expression (2.7 ± 0.1 fold) of the *cj0411* gene in the *frdA* mutant compared with the wild-type parent strain, showing that there was no negative effect on this gene resulting from the *frdA* insertion. The genes downstream of the *mfr* operon are transcribed from the opposite DNA strand and so potential polar effects of the *mfrA* mutation will not disrupt their transcription.

Disruption of *mfrA* had no effect on microaerobic growth in complex media, with both growth rate and final cell yields being identical to wild-type (Fig. 2A). In contrast, growth of the *frdA* mutant strain was poor and stopped after a few hours (Fig. 2B). However, the addition of 20 mM sodium fumarate to microaerobic cultures of the *frdA* mutant resulted in slow exponential growth (doubling time of 6 h) and a final cell yield similar to that of the wild-type after 24 h (Fig. 2B). The growth of the wild-type and *mfrA* mutant were unaffected in fumarate-supplemented media (data not shown). Results with the double *frdA mfrA* mutant (Fig. 2C) were identical to those with the single *frdA* mutant, showing that the fumarate-dependent growth stimulation is not due to the activity of the Mfr enzyme.

To investigate the roles of the Mfr and Frd systems in the utilization of fumarate as an alternative electron acceptor, growth of the mutants was investigated under oxygen-limited conditions generated in unshaken batch cultures in filled culture bottles as described in *Experimental procedures* and previously (Sellars *et al.*, 2002; Guccione *et al.*, 2008). In the absence of fumarate in the media, none of the strains showed any growth. In the presence of 40 mM sodium fumarate as electron acceptor, the wild-type strain grew well (doubling time of 4 h), while the *mfrA* mutant grew at a reproducibly slower rate (doubling time of 7 h) than wild-type but reached a similar final cell yield (Fig. 2A). In contrast, the *frdA* and *frdA mfrA*

mutants showed no detectable growth above that of a no-fumarate control (Fig. 2B and C).

Both Frd and Mfr have fumarate reductase activity but succinate oxidation is catalysed by Frd alone

Total fumarate reductase activity was assayed in intact cells using the membrane permeable benzyl viologen radical (Sellars *et al.*, 2002). Wild-type cells grown to early stationary phase (16 h) in complex media showed a high rate ($\sim 1 \mu\text{mol min}^{-1} \text{mg protein}^{-1}$) of fumarate-dependent oxidation of reduced benzyl viologen. Both the *mfrA* mutant and the *frdA* mutant exhibited reductions in activity but to significantly different extents. The *mfrA* mutant showed an average 40% reduction in activity compared with wild-type ($P < 0.05$), while the *frdA* mutant showed an approximate 90% reduction compared with the wild-type (see Fig. 3A). The *frdA mfrA* double mutant displayed no activity in this assay. These data show that the Frd and the Mfr complexes together account for all of the cellular fumarate reductase activity, and that under the growth conditions used, most of the activity in wild-type cells is contributed by the Frd enzyme. However, the fact that the *frdA* mutant still exhibits residual activity, and the *mfrA* mutant shows a significant decrease, indicates that the fumarate reductase activity of the Mfr enzyme is detectable *in vivo* in *C. jejuni*.

Succinate dehydrogenase assays were performed by measuring succinate-dependent reduction of dichlorophenolindophenol (DCPIP) dye in cell-free extracts (see Fig. 3B). The specific activity in the *mfrA* mutant ($112.1 \pm 4.7 \text{ nmol min}^{-1} \text{mg protein}^{-1}$) was not statistically different to the isogenic wild-type ($122.6 \pm 3.1 \text{ nmol min}^{-1} \text{mg protein}^{-1}$; $P > 0.05$). However, the *frdA* mutant showed a virtual complete loss of activity in this assay ($2.4 \pm 2.3 \text{ nmol min}^{-1} \text{mg protein}^{-1}$), as did the *frdA mfrA* double mutant ($1.3 \pm 1.6 \text{ nmol min}^{-1} \text{mg protein}^{-1}$). These data are consistent with those from succinate-dependent oxygen respiration assays in intact cells (shown in Fig. 3C). When succinate was provided as an electron donor in an oxygen electrode, respiration rates of the *mfrA* mutant were not significantly different to those of the wild-type strain ($P > 0.05$), but neither the *frdA* mutant nor the *frdA mfrA* double mutant respired succinate. All strains respired formate at rates of $> 300 \text{ nmol min}^{-1} \text{mg protein}^{-1}$. Taken together, the enzyme and oxygen uptake data show that succinate respiration is dependent only on Frd and not the Mfr complex.

Periplasmic localization of MfrA and MfrB subunits and accumulation of unprocessed MfrA in the cytoplasm of an mfrE mutant

In order to confirm the cellular location of the Mfr enzyme encoded by *cj0437–0439* in *C. jejuni* NCTC 11168, we

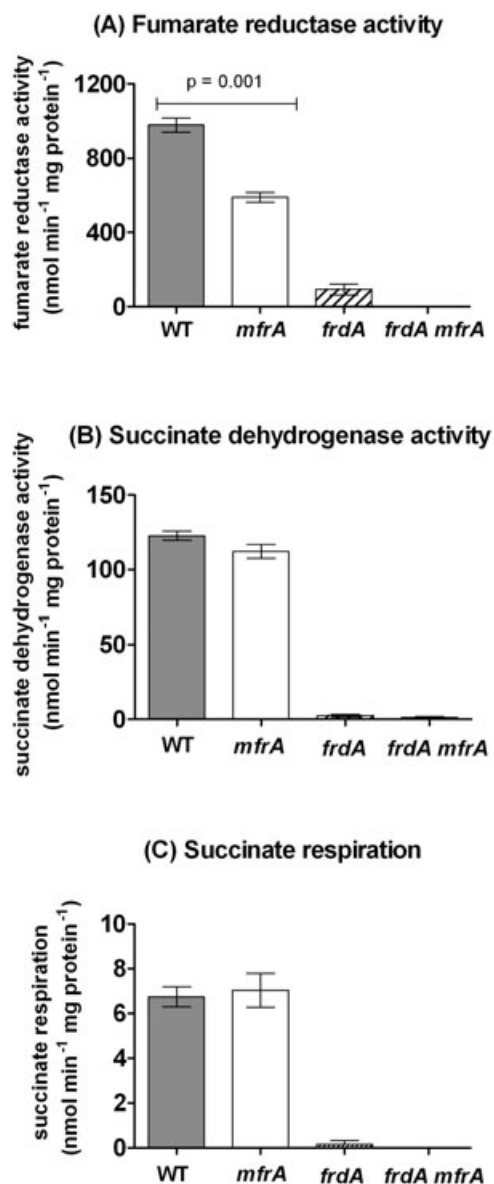


Fig. 3. Fumarate reductase and succinate dehydrogenase activities in wild-type and mutant strains.

A. Fumarate reductase activities in intact wild-type and mutant cells, which were grown to early stationary phase in BHI-FCS, measured using reduced benzyl viologen as an artificial electron donor.

B. Succinate dehydrogenase activities in cell-free extracts of wild-type and mutant strains assayed using oxidized DCPIP as an artificial electron acceptor.

C. Succinate-dependent oxygen respiration in wild-type and mutant intact cells grown to early stationary phase in BHI-FCS. In all cases, error bars represent the standard error of the mean of at least three biological replicates. Statistical significance was analysed by Student's *t*-test.

fractionated cells to prepare periplasm as previously described (Myers and Kelly, 2005; Atack *et al.*, 2008) using cells grown under standard microaerobic conditions to stationary phase. As shown in Fig. 4A, periplas-

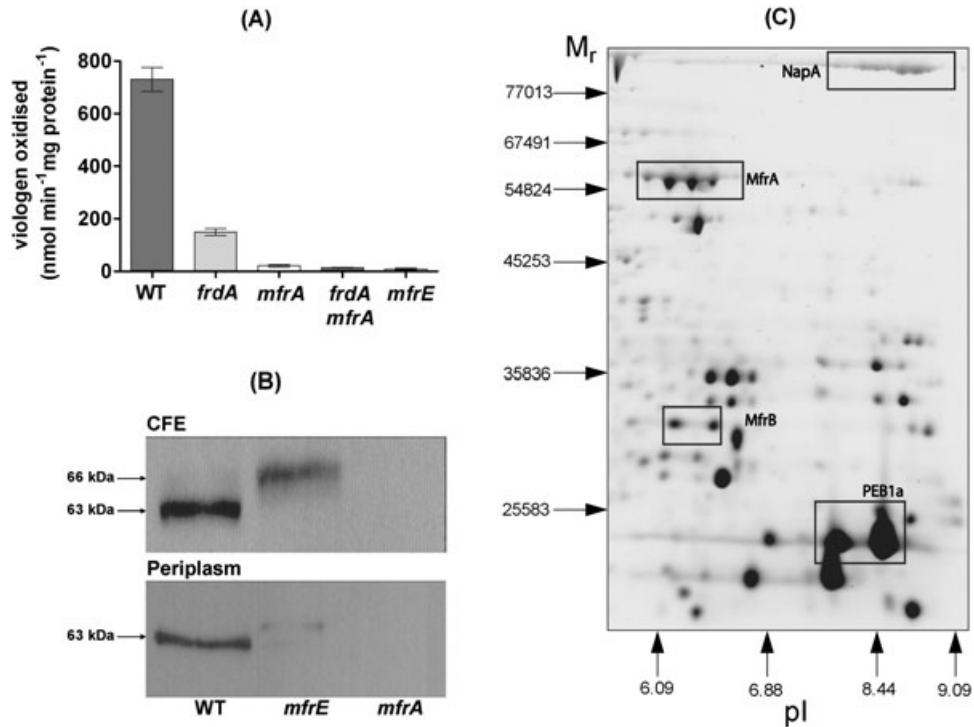


Fig. 4. Periplasmic localization of MfrA/MfrB and mislocalization of MfrA in an *mfrE* mutant.

A. Fumarate reductase activity in wild-type and mutant periplasmic fractions. Benzyl viologen was utilized as an artificial electron donor. B. Western blot analysis of wild-type, *mfrA* and *mfrE* mutant cell-free extracts (CFE) and periplasm with anti-MfrA antibody. Approximately 20 µg of protein was loaded in each lane.

C. Separation of wild-type periplasmic proteins by 2D-gel electrophoresis followed by mass spectroscopic identification of protein spots. Mowse scores supporting the identification of MfrA isoforms were 203, 291, 169 and 344. Scores for identification of MfrB isoforms were 211 and 196. Mowse scores greater than 56 are significant ($P < 0.05$).

mic fractions of wild-type but not *mfrA* mutant cells exhibited significant fumarate reductase activity, while periplasm from *frdA* mutant cells retained about 20% of the wild-type activity. As expected, periplasm prepared from the *frdA mfrA* double mutant displayed no activity. It is not clear why the Mfr-dependent activity in the *frdA* mutant is lower than that of the wild-type, but this mutant is very slow-growing. Western immunoblots using anti-MfrA antibody prepared in rats showed that the MfrA subunit was easily detectable in cell-free extracts of the wild-type but not *mfrA* mutant (Fig. 4B). The antibody did not cross-react with FrdA. In the corresponding periplasmic fractions, the same pattern was seen but the MfrA band in the wild-type was weaker. Presumably, most of the MfrA subunits are bound to the membrane via MfrB and the membrane anchor MfrE, limiting the amount of free MfrA in the periplasm detectable by blotting or activity measurements. Separation of wild-type periplasmic proteins by 2D-gel electrophoresis (Fig. 4C), followed by mass spectroscopic identification of protein spots after tryptic digestion, identified both MfrA (4 isoforms) and MfrB (2 isoforms) to be present, along with a number of

known marker proteins that have previously been established by us to be located in the periplasm. These include NapA (Pittman *et al.*, 2007) and the aspartate/glutamate solute binding-protein PEB1a (Leon-Kempis *et al.*, 2006).

mfrE encodes the unusual membrane-associated electron transfer subunit that is unique to the E-type class of SQORs. An *mfrE* insertion mutant was constructed and tested for growth and production of MfrA by activity measurements and immunoblotting. The *mfrE* mutant grew normally microaerobically, but showed the same slight growth defect under oxygen-limited conditions as the *mfrA* mutant (Fig. 2D), which could be consistent with an essential role of MfrE in electron transport through the enzyme to MfrA. Interestingly however, immunoblotting with anti-MfrA antibody showed a higher molecular mass form of MfrA was present in total cell-extracts of the *mfrE* mutant compared with the wild-type (Fig. 4B), but only a faint band was present in the periplasm. This probably represents a small amount of cytoplasmic contamination, as essentially no viologen-dependent MfrA activity could be detected in the *mfrE* mutant periplasm (Fig. 4A). These

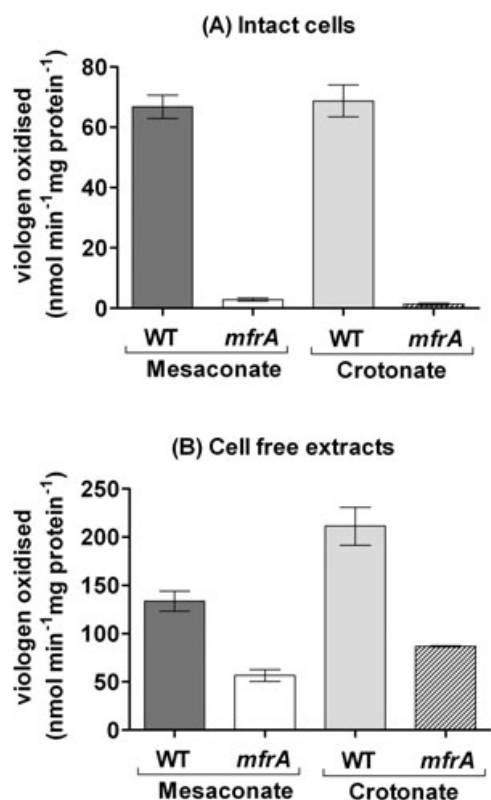


Fig. 5. MfrA-dependent reduction of mesaconate and crotonate. A. Assays of mesaconate and crotonate reductase activity in intact wild-type and *mfrA* mutant cells, measured using reduced benzyl viologen as an artificial electron donor. B. Corresponding activities in cell-free extracts. In all cases, error bars represent the standard error of the mean of three biological replicates.

data and the ~3 kDa increased size of the MfrA protein in the *mfrE* mutant suggests that the absence of MfrE causes cytoplasmic accumulation of the unprocessed form of MfrA, i.e. retaining its TAT signal sequence.

Mfr reduces the fumarate analogues mesaconate and crotonate

Intact cells of the wild-type and *mfrA* mutant were tested in the benzyl viologen assay for their ability to reduce a range of unsaturated mono- and dicarboxylate analogues of fumarate. In addition to fumarate, wild-type but not *mfrA* mutant cells reduced mesaconate (2-methylfumarate) and crotonate (2-butenate). Glutaconate, cinnamate and maleate were not reduced. The rates of mesaconate and crotonate reduction were about 30-fold lower than fumarate reduction at the same substrate concentrations (Fig. 5A). Given the cytoplasmic location of the active site of Frd, the observation that *mfrA* mutant cells were unable to reduce these alternative substrates does not exclude the possibility that they could be reduced by Frd, but are unable to cross the cytoplasmic membrane. In order to

test this, cells of the *mfrA* mutant were sonicated and cell-free extracts assayed for reductase activity. As shown in Fig. 5B, an increase in relative activity was noted in the mutant versus wild-type extracts, but there remained a significant difference in activities between wild-type and *mfrA* cell-free extracts. The data suggest that although Frd may be able to reduce mesaconate and crotonate to some extent, these substrates are unlikely to be transported into the cell, and therefore in intact cells can only be reduced by Mfr in the periplasm. This hypothesis was further tested by ¹H-NMR spectroscopy of supernatants from cells of wild-type and *mfrA* mutants incubated with fumarate or mesaconate under oxygen-limited conditions and sampled at intervals (Fig. 6). As expected, fumarate was reduced rapidly by wild-type cells and stoichiometric amounts of succinate were produced, but the *mfrA* mutant showed a clear reduction in the rate of fumarate consumption and succinate production (Fig. 6A). In agreement with the viologen activity assays, wild-type cells reduced mesaconate more slowly than fumarate but eventually accumulated the reduction product 2-methylsuccinate to a concentration stoichiometric with the starting mesaconate concentration (Fig. 6B). Significantly, over the time-course of the assay, no net mesaconate reduction or 2-methylsuccinate production could be detected in the *mfrA* mutant supernatants (Fig. 6B), confirming that mesaconate reduction in intact cells is entirely due to the periplasmic Mfr enzyme.

mfrA is highly upregulated after an oxygen downshift in chemostat culture

In many bacteria fumarate reductases are anaerobically inducible enzymes due to their role in providing an alternative electron transport pathway in the absence of oxygen. The regulation of expression of the *frdA* and *mfrA* genes with respect to oxygen was investigated by quantitative RT-PCR analysis before and after an oxygen downshift, using cells maintained in steady-state under carefully controlled continuous culture conditions in a chemostat. The cells were grown at a dilution rate (= growth rate) of 0.2 h⁻¹ in carbon (serine)-limited defined media at an initial input gas composition of 10% v/v oxygen/10% v/v carbon dioxide/80% v/v nitrogen (cell density of 0.3 mg dry weight ml⁻¹; yield = 38 g cells mol⁻¹ serine). At time 0, the culture was made anaerobic by switching the gas mixture to 0% v/v oxygen/10% v/v carbon dioxide/90% v/v nitrogen. Cell samples were taken prior to the shift and at timed intervals afterwards, and processed for RNA extraction and RT-PCR analysis. The results (Fig. 7A) reveal a dramatic increase in expression of the *mfrA* gene upon anaerobiosis to > 200-fold compared with preshift aerobic conditions. The *frdA* gene was also anaerobically inducible, but to a much lesser

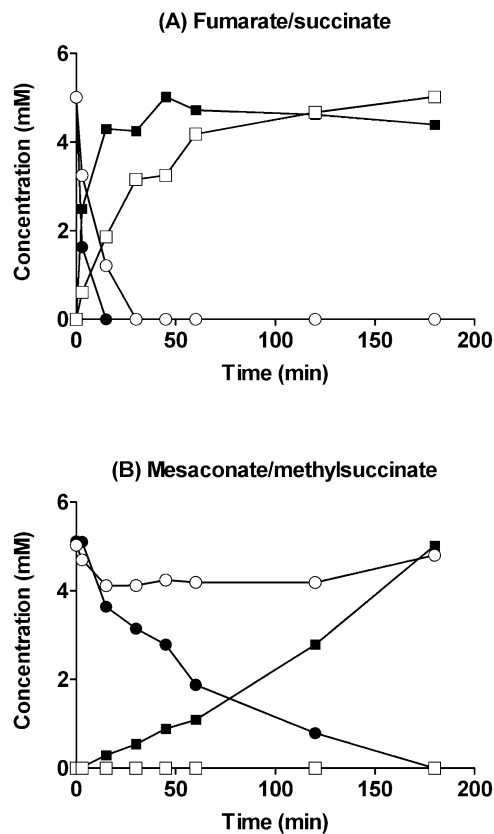


Fig. 6. $^1\text{H-NMR}$ analysis of (A) fumarate and (B) mesaconate reduction in intact cells. An incubation mixture consisting of 20 ml defined minimal media (Table S1) without serine but with 20 mM sodium formate (electron donor) and either 5 mM fumarate (A) or 5 mM mesaconate (B) as electron acceptor was sparged with oxygen-free nitrogen, incubated unshaken at 37°C in a sealed vessel with minimal headspace and inoculated at time zero with an equivalent cell mass (final cell density $2 \text{ mg dry weight ml}^{-1}$) of either wild-type or *mfrA* mutant cells harvested from overnight microaerobically grown cultures in MH-S media. At timed intervals, samples (1 ml) were removed, centrifuged to remove cells, and the supernatants frozen in liquid nitrogen for subsequent NMR analysis to quantify substrate and product concentrations (see *Experimental procedures*). Filled symbols; wild-type. Open symbols; *mfrA* mutant. Circles show concentration of either fumarate (A) or mesaconate (B) and squares show concentration of succinate (A) or 2-methylsuccinate (B).

maximal extent (c. sixfold). However, the absolute abundance of the *frdA* mRNA was much higher than that of the *mfrA* mRNA (Fig. 7B), reflecting the differences in activities seen in the enzyme assays described above. Cell samples taken before and post shift were also assayed for total fumarate reductase activity, which revealed a sixfold increase after 2.5 h (Fig. 7C). In this experiment, no exogenous fumarate was present in the media, as we wanted to specifically determine the effect of oxygen. However, separate assays have shown that the presence or absence of fumarate in growth media has a minimal effect on the total fumarate reductase activity.

Discussion

The mutant growth data show that the Frd complex is essential both for normal aerobic growth and also for fumarate respiratory growth, while the Mfr complex is not needed for growth with oxygen as terminal electron acceptor but is necessary to allow maximal growth rates to be achieved with fumarate as an electron acceptor

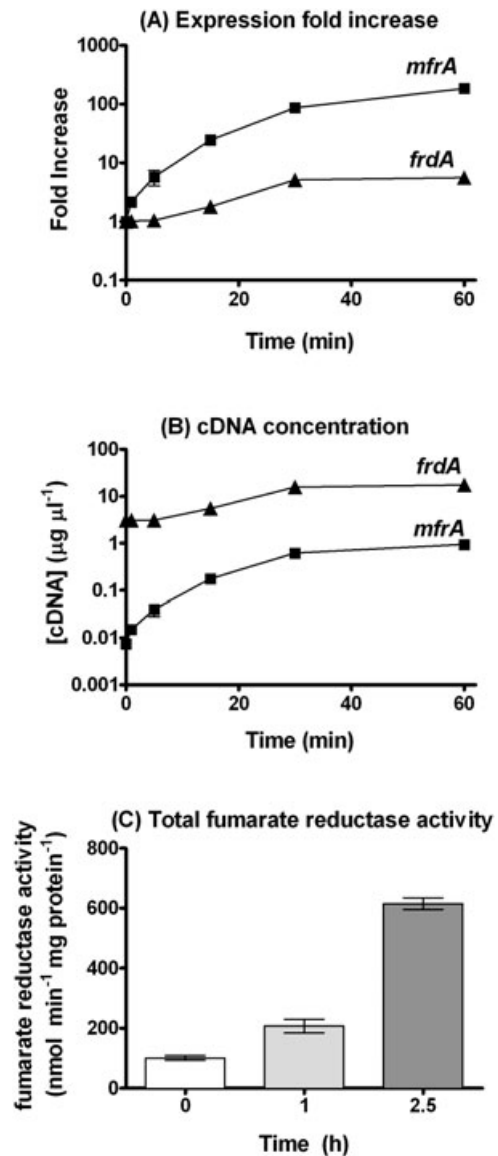


Fig. 7. Upregulation of *mfrA* and *frdA* in wild-type *C. jejuni* in response to a transition from microaerobic to anaerobic conditions in chemostat culture. Quantitative RT-PCR was used to determine the fold increase (A) and absolute concentration (B) of *mfrA* and *frdA* cDNA in response to an aerobic to anaerobic transition in defined media (serine-limited, no fumarate added) in a chemostat at a dilution rate of 0.2 h^{-1} (see *Experimental procedures* for details). (C) Total fumarate reductase activity of intact cells after the shift measured using reduced benzyl viologen as electron donor. In all cases, error bars represent the standard error of the mean of three biological replicates.

under low oxygen conditions. An analysis of the abilities of the *mfrA* and *frdA* mutants to reduce fumarate and oxidize succinate confirmed that in *C. jejuni*, it is the Frd complex and not the 'Sdh' complex, which is essential for succinate oxidation, and therefore, functions as part of the TCA cycle. This explains the marked growth defect of the *frdA* mutant under microaerobic conditions. Thus, it appears that in *C. jejuni* FrdABC is a bifunctional complex that catalyses both fumarate reduction and succinate oxidation *in vivo*. Although many SQORs are capable of catalysing both fumarate reduction and succinate oxidation (Cecchini *et al.*, 2002; Hederstedt, 2002), they rarely seem to function bidirectionally *in vivo*. However, Butler and colleagues (2006) showed that *Geobacter sulphurreducens* performs both functions with a single enzyme. Supplying exogenous fumarate to mutant strains of *G. sulphurreducens* lacking this enzyme restored aerobic growth because the bacterium uses the TCA cycle only for anabolic purposes, while oxidizing iron for energy conservation. Interestingly, fumarate was able to significantly improve aerobic growth of the *C. jejuni frdA* mutant, although it did not result in restoration of wild-type rates of growth. This growth stimulation was independent of Mfr, as the *frdA mfrA* double mutant showed the same phenotype as the *frdA* mutant. A catabolic pathway that converts fumarate to pyruvate via malic enzyme and then to acetate via the *por*, *pta* and *ackA* genes could be responsible for the slow fumarate-dependent aerobic growth of the *frdA* mutant. This pathway can generate up to one mole ATP per mole of pyruvate (Kelly, 2008).

Unlike the situation reported in *W. succinogenes* by Juhnke and colleagues (2009), viologen-linked fumarate reductase activity due to catalysis by MfrA was detectable in periplasmic extracts of *C. jejuni*, and immunoblot and proteomic analysis of such extracts showed the presence of MfrA and MfrB subunits. However, the MfrB subunit does not contain a TAT sequence, so it is likely that it is co-translocated along with MfrA by the 'hitch-hiker' mechanism that has been found in some other TAT substrate enzyme complexes (Berks *et al.*, 2005). Furthermore, an *mfrE* mutant accumulated unprocessed MfrA in the cytoplasm, which would be consistent with MfrE being essential for correct transport of MfrA through the TAT system. Taken together, the data suggest an assembly pathway for the holoenzyme in which the entire MfrABE complex is formed in the cytoplasm, then recognized and transported to the periplasm in a TAT-dependent manner using only the MfrA twin-arginine sequence, followed by association of the holoenzyme with the membrane via MfrE.

The *C. jejuni mfrABE* operon is transcribed from a single σ^{70} -dependent promoter (Petersen *et al.*, 2003), which was located unexpectedly far upstream of the *mfrA* start codon. Inspection of the *mfrA* 5' UTR sequence

indicated that it contained an ORF putatively encoding a small polypeptide of 60 amino acids, which contains a single transmembrane domain. Initial annotation of genome sequences often used a cut-off value of >100 amino acids for ORFs, and it has recently become apparent that the intergenic regions in bacterial genomes can contain many small ORFs encoding membrane proteins (Hemm *et al.*, 2008); this seems also to be the case in *C. jejuni*. Homology searches with the polypeptide encoded by the small ORF (tentatively named *mfrX*) showed that it is conserved in all *C. jejuni* strains and in *C. doylei*, but homologues are not present in other bacterial genome sequences available. Whether the protein encoded by the small ORF has any function in MfrABE enzyme function or biogenesis is unclear, as we could find no obvious phenotype for an *mfrX* mutant and the mutant still produced MfrA. The 5' RACE experiments suggest that there may be post-transcriptional processing of the *mfrX-mfrABE* mRNA towards higher stability of a transcript containing only *mfrABE*, which may be required in larger amounts than the polypeptide encoded by *mfrX*.

While the FrdABC complex clearly acts in both succinate oxidation and in fumarate reduction, the physiological role of the MfrABE complex as an additional fumarate reductase and the rationale for a periplasmic location was not immediately obvious. The reduction of fumarate in the periplasm means that the Mfr enzyme is non-electrogenic, but it is now clear that the Frd enzyme in epsilon-proteobacteria also operates in a non-electrogenic manner due to the un-coupling 'E-pathway' (Lancaster *et al.*, 2005), and thus (with fumarate as substrate) there appears to be no difference in the overall energetics of the two complexes. We found, however, that Mfr does contribute to fitness under fumarate-dependent growth conditions, as evidenced by the slight oxygen-limited growth defect of the *mfrA* and *mfrE* mutants and slower fumarate reduction kinetics in the absence of MfrA (Fig. 6A), although its activity in the *frdA* mutant background appears insufficient alone to support any significant growth. Possibly, the periplasmic Mfr allows more rapid adaptation to fumarate-dependent growth, as coupled fumarate transport and succinate efflux through the DcuA and DcuB systems is required, before fumarate reduction can be catalysed by Frd (Fig. 8). The gene expression studies described above clearly show that the *mfr* genes are very highly upregulated by oxygen limitation, which would be consistent with such a role. In addition, previous studies have revealed that these genes are upregulated 15- to 30-fold in bacteria growing in the caeca of 1-day-old chicks compared with broth grown controls (Woodall *et al.*, 2005), suggesting a role *in vivo*.

We also considered the possibility that the Mfr enzyme uses alternative substrates in addition to fumarate, which

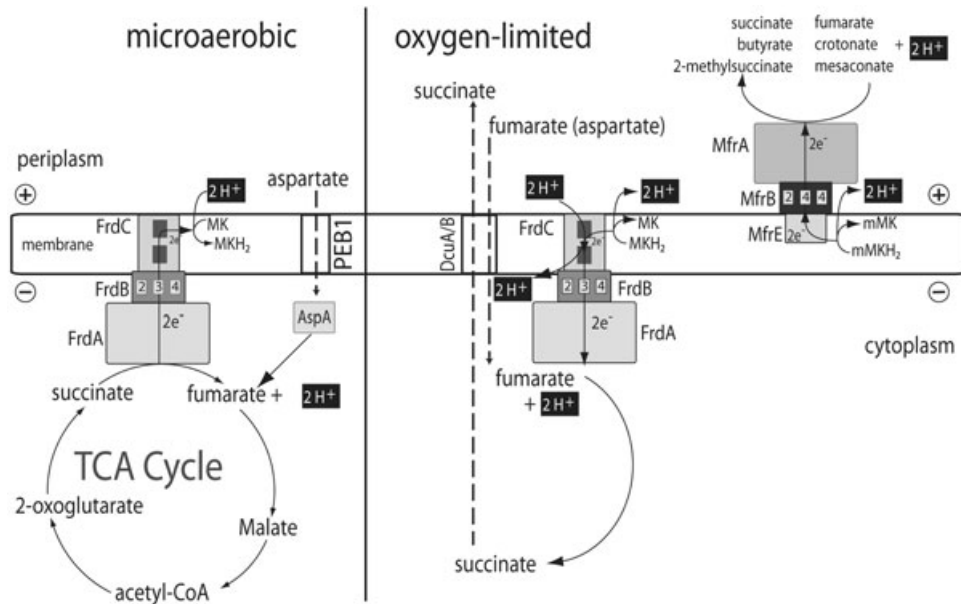


Fig. 8. A model for the operation of FrdABC and MfrABE in *C. jejuni*. The left hand side of the figure shows the role of the bifunctional FrdABC complex under microaerobic conditions. FrdABC acts as a TCA cycle enzyme converting succinate to fumarate and donating electrons to the menaquinone (MK) pool. Under oxygen-limited conditions (right hand side of diagram) the FrdABC complex acts as a fumarate reductase, accepting electrons from the MKH₂ pool. This is an electroneutral process due to the translocation of protons by the 'E-pathway' (Lancaster *et al.*, 2005). As the MfrABE complex is periplasmic, substrate reduction coupled to quinol oxidation will also be electroneutral. MfrABE is likely to be translocated as a preformed complex to the periplasm via the TAT system and acts as a methylmenaquinol (mMKH₂) dependent C4-mono/di-carboxylic acid reductase with a preference for fumarate. It is also able to reduce mesaconate and crotonate, substrates that cannot easily cross the cytoplasmic membrane. Numbers within boxes in the FrdB and MfrB subunits refer to differences in the iron-sulfur centres in these proteins, either 2Fe-2S [2], 3Fe-4S [3] or 4Fe-4S [4] (see Lemos *et al.*, 2002).

might be consistent with the observation (Lemos *et al.*, 2002) that a normally highly conserved residue at the subunit A dicarboxylate binding site, Phe141, is changed to Met in *C. jejuni* and to Ala in *W. succinogenes*. The C4-dicarboxylate mesaconate and the C4-monocarboxylate crotonate were clearly identified as alternative substrates. Mesaconate is an intermediate in glutamate fermentation via the 3-methylaspartate pathway in various common gut anaerobes such as *Clostridium*, *Fusobacterium* and *Eubacterium* species (Buckel, 2001). Crotonate is also an intermediate in anaerobic substrate transformations that is known to be utilized by a range of anaerobic bacteria (Bader *et al.*, 1980). These substrates are thus potentially available to *C. jejuni* in the avian caecum or mammalian intestine as a result of the activity of anaerobic commensals with which *C. jejuni* shares its niche. Interestingly, our data suggest that although Frd can reduce mesaconate and crotonate to some extent, these electron acceptors do not appear to be transported across the cytoplasmic membrane of *C. jejuni*, providing a further rationale for the periplasmic location of a reductase able to reduce such compounds. In addition, although the midpoint redox potentials of the fumarate/succinate and mesaconate/methylsuccinate couples are likely to be very similar (about +30 mV), that of the crotonate/butyrate couple can be calculated to be

–24 mV, using the ΔG° value of -75 kJ mol^{-1} for crotonate reduction given in Thauer and colleagues (1977). This is only about 50 mV higher than the MK/MKH₂ couple (–75 mV), but 100 mV higher than the mMK/mMKH₂ couple (–124 mV). Therefore, there may well be some kinetic advantage in having a greater driving force for crotonate reduction by mMKH₂ than by MKH₂. Our data also do not exclude the possibility that Mfr can use additional substrates with redox potentials approaching or even below that of the MK/MKH₂ couple, in which case only reduction by mMKH₂ would be thermodynamically favourable.

During preparation of this manuscript, a study on the *C. jejuni* Frd enzyme was published (Weingarten *et al.*, 2009). These authors independently noticed the microaerobic growth defect of an *frdA* mutant and the role of Frd as a succinate dehydrogenase, but did not test growth under oxygen-limited conditions. Although their *frdA* mutant colonized chickens slightly less well than the wild-type, given its large growth defect these results are difficult to interpret. Interestingly, an *mfrA* mutant did not have a chicken colonization defect (Weingarten *et al.*, 2009). However, in view of our data, it would be worthwhile to test the colonization of an *frdA mfrA* double mutant, as this will not have any alternative fumarate reductase pathway.

A model of the function and organization of the Frd and Mfr complexes of *C. jejuni*, based on the work described here and our previous work (Guccione *et al.*, 2008), is shown in Fig. 8. This model shows the dual functionality of the cytoplasmic facing Frd enzyme, which acts as a succinate dehydrogenase under conditions of adequate aeration but is also responsible for the majority of fumarate reduction in cells that are oxygen-limited. The periplasmic facing Mfr complex is highly inducible under low-oxygen conditions and acts as an additional fumarate reductase that may allow more rapid adaptation to fumarate respiration, but may also have a role in the reduction of alternative substrates such as mesaconate and crotonate, which are unable to be transported across the cytoplasmic membrane. Our data add to an emerging picture of a surprising complexity in periplasmic electron transfer reactions in *C. jejuni* (Kelly, 2008), many of which appear to be crucial to growth in the host, for example gluconate oxidation (Pajaniappan *et al.*, 2008), nitrate and nitrite reduction (Pittman *et al.*, 2007; Weingarten *et al.*, 2008), and hydrogen and formate oxidation (Weerakoon *et al.*, 2009).

Experimental procedures

Bacterial strains, media and batch culture conditions

Campylobacter jejuni strain NCTC 11168 was routinely grown at 37°C under microaerobic conditions [10% (v/v) O₂, 5% (v/v) CO₂ and 85% (v/v) N₂] in a MACS-VA500 incubator (Don Whitley Scientific, UK) on Columbia agar (CA) containing 5% (v/v) lysed horse blood and 10 µg ml⁻¹ each of amphotericin B and vancomycin. To select *C. jejuni* mutants, kanamycin (Km) or chloramphenicol (Cm) was also added, to a final concentration of 30 µg ml⁻¹. Liquid cultures of *C. jejuni* for growth curves were grown in Müller–Hinton (MH), or brain–heart infusion (BHI) broth supplemented with 5% (v/v) foetal calf serum (BHI-FCS), and appropriate antibiotics at 37°C, under (i) standard microaerobic conditions (gas concentrations as above) with 50 ml of medium contained in 250 ml conical flasks, mixed by continuous orbital shaking at 120 r.p.m., or (ii) oxygen-limited conditions, where the gas atmosphere was as in (i) but where the diffusion of oxygen was severely restricted by using 500 ml medium contained in a 500 ml conical flask as described previously (Sellars *et al.*, 2002). Fumarate was added to the media from filter-sterilized stock solutions to a final concentration of 20–40 mM. Growth curves shown are representative of single experiments, but all growth experiments were repeated several times with similar results. Media for all growth experiments was pre-incubated in a microaerobic gas-atmosphere for 24 h at 37°C before inoculation with a microaerobically grown BHI-FCS starter culture. Growth was monitored by measuring optical density at 600 nm in an Ultrospec 2000 spectrophotometer (Amersham Pharmacia Biotech, UK). *Escherichia coli* DH5α (Stratagene, UK) and Origami™ B(DE3) (Novagen, UK) strains were cultured in Luria–Bertani (LB) medium supplemented with appropriate antibiotics at 37°C.

Continuous chemostat culture

Campylobacter jejuni NCTC 11168 cells were grown in a carbon (serine)-limited chemostat (Infors HT Labfors 3 monitored and controlled using Infors Iris 5 software; Infors, Switzerland) in a specially designed defined medium based on MEM-α medium (see Table S1) initially under microaerobic conditions (input gas composition: 10% v/v oxygen, 10% carbon dioxide and 80% nitrogen) at 37°C. The culture volume was 885 ml, the gas sparging rate was 0.5 l min⁻¹ with a stirring rate of 350 r.p.m and the pH was maintained at 7 ± 0.1 with automatic addition of 1 M NaOH or H₂SO₄. Dissolved oxygen was measured using a Bradley James D100 probe. After inoculation, cells were initially grown as a batch culture for 6 h, reaching an OD₆₀₀ of ~0.6; at this point fresh media were fed into the vessel at a dilution rate of 0.2 h⁻¹, until steady state was reached, defined by a stable cell density for >5 vessel volumes of fresh media supplied to the chemostat. Samples were taken from the chemostat in steady state, then the gas mixture changed to 10% CO₂/90% N₂, and further samples taken at 1, 5, 15, 30, 60 and 150 min after anaerobiosis was imposed. The changes in expression of *frdA* and *mfrA* in these samples were measured using SYBR green quantitative RT-PCR (qRT-PCR) as described below.

DNA isolation and manipulation

Plasmid DNA was isolated using Qiagen Miniprep kits (Qiagen, UK). *Campylobacter jejuni* genomic DNA was extracted using a MicroLysis kit (Web Scientific, UK). Standard techniques were employed for the cloning, transformation, preparation and restriction analysis of plasmid DNA from *E. coli* (Sambrook *et al.*, 1989).

Overexpression and purification of MfrA

PCR primers *mfrAOE-F* and *mfrAOE-R* (Table S2) were designed to amplify the entire coding region of *Cj0437* for cloning into pET21a (Merck Chemicals, UK) under the control of the isopropyl-β-D-thiogalactopyranoside (IPTG) inducible T7 promoter. The gene was amplified from *C. jejuni* NCTC 11168 chromosomal DNA using *Accuzyme* DNA polymerase (Biolone, UK). The PCR product was cloned into the EcoRI site of pGEM®3Zf(-) (Promega, UK), excised with a NdeI-XhoI digest, then directionally cloned into similarly restricted pET21a. Automated DNA sequencing (MRC Centre for Developmental and Biomedical Genetics, Sheffield, UK) showed that the sequence of the cloned gene was correct. Plasmids were transformed into *E. coli* Origami™ B(DE3) (Novagen, UK), which was grown aerobically at 37°C in LB medium containing carbenicillin (50 µg ml⁻¹) and riboflavin (5 mg ml⁻¹). At an OD₆₀₀ of 0.6, 1 mM IPTG was added, and the induced cells were grown for 24 h at 25°C before harvesting by centrifugation (8000 g, 10 min, 4°C). Cell pellets containing overexpressed protein were disrupted by sonication with a MSE Soniprep 150 (Sanyo, UK) using 3 × 20 s bursts of ultrasound (amplitude ~16 microns peak to peak) with 30 s intervals between bursts and the soluble fraction isolated as the supernatant after centrifugation (16 000 g, 15 min, 4°C). FAD was added at this step to a final concen-

tration of 500 μM along with a protease inhibitor cocktail (Sigma, UK; 0.5 ml g^{-1} of cell paste). Cell extracts were fractionated on a HisTrap FF crude 1 ml column (GE Healthcare, UK) by affinity chromatography. Protein was bound to the column in 50 mM Tris-HCl buffer pH 8.0 containing 0.5 M NaCl and eluted from the resin by a linear gradient from 0 to 250 mM imidazole in the same buffer. Fractions were pooled and adjusted to 1.5 M ammonium sulfate and further fractionated by hydrophobic interaction chromatography using a 1 ml Resource™ ISO column (GE Healthcare, UK). Elution was achieved by a salt gradient of 1 to 0 M ammonium sulfate. Protein was concentrated as desired using a VivaSpin column with a 30 000 molecular weight cut off (VivaScience, UK) and ammonium sulfate was removed using a diafiltration cup or dialysis. The MfrA protein was judged to be pure by Coomassie blue staining on overloaded SDS-PAGE gels.

Construction and complementation of *C. jejuni* mutants

The *frdA* gene (1992 bp) was amplified using the *frdAM*-F and *frdAM*-R primers (Table S2) creating a 2047 bp product that was inserted at the XbaI and SphI sites of pGEM3ZF (Promega, UK) to create pEJG8. A non-polar chloramphenicol acetyl-transferase (*cat*) cassette derived from *Campylobacter coli* (contained in plasmid pAV35; van Vliet *et al.*, 1998) was inserted at a unique EcoRV site in the *frdA* coding region in the same transcriptional orientation to create pEJG9. For mutagenesis of *mfrA*, the coding region was amplified by PCR using the primers *mfrAM*-F and *mfrAM*-R (Table S2) to give a 1.9 kb PCR product that was inserted at the XbaI and SphI sites of pGEM3ZF. The resulting plasmid (pEJG10) was linearized with EcoRV, which cuts uniquely within the *mfrA* gene, and, the *cat* cassette from pAV35 inserted as above, creating the 6 kb pEJG11 plasmid. In order to construct a double *mfrA frdA* mutant, a further plasmid (pEJG12) was made by inserting the non-polar *aphAIII* (*kan*) gene from *C. coli* (Wang and Taylor, 1990; van Vliet *et al.*, 1998), encoding kanamycin resistance, into the EcoRV site of pEJG10. The *mfrE* gene and flanking upstream sequence was amplified using primers *mfrEM*-F and *mfrEM*-R (Table S2) to generate a 1258 bp product that was inserted into the XbaI and BamHI sites of pET-9a (Merck Chemicals, UK), creating plasmid pAH439a. The non-polar *cat* cassette from pAV35 was inserted as above at a unique ScaI site in the *mfrE* coding region to create the construct pAH439b. Transformation of *C. jejuni* NCTC 11168 with plasmids pEJG9, pEJG11 and pAH439b was carried out by electroporation, and transformants were selected on CA plates supplemented with chloramphenicol at a final concentration of 30 $\mu\text{g ml}^{-1}$. A double *frdA mfrA* mutant was constructed by electrotransformation of the *frdA::cat* mutant with pEJG12 and selection on CA plates with both kanamycin and chloramphenicol. Putative transformant colonies were re-streaked onto CA plates and correct insertion of the antibiotic resistance cassettes into the target genes was verified by extraction of chromosomal DNA by the MicroLYSIS kit (Web Scientific, UK) according to manufacturer's instructions. PCR using the gene-specific primers listed above confirmed allelic exchange by double cross-over, as demonstrated by an increase in amplicon size of approximately 0.9 or 1.4 kb for the chloramphenicol or kanamycin cassette insertions

respectively. For complementation of *frdA* and *mfrA* mutants, primers *frdACOMP*-F and *frdACOMP*-R, and *mfrACOMP*-F and *mfrACOMP*-R (Table S2), were used to amplify the wild-type NCTC 11168 genes, which were cloned into the XbaI site of plasmid pRRK (Karlyshev and Wren, 2005), such that transcription was driven by the promoter of the kanamycin resistance gene. The plasmids were electrotransformed into mutant strains with selection on CA plates plus kanamycin.

For construction of an *mfrX* mutant, primers *mfrX5*-F and *mfrX5*-R (Table S2) were used to PCR amplify 12 bp of the 5' end of *mfrX* plus 430 bp of upstream DNA (fragment A). The reverse primer included a linker region with a BamHI restriction site. Primers *mfrX3*-F and *mfrX3*-R (Table S2) were used to amplify 140 bp of the 3' end of *mfrX* plus 304 bp of downstream DNA (fragment B). The forward primer contained a linker complementary to that used in the amplification of fragment A. A second PCR, using both fragments A and B as template with primers *mfrX5*-F and *mfrX3*-R, resulted in a single amplicon, in which 31 bp of *mfrX* were replaced with a linker containing a BamHI restriction site. This amplicon was cloned into pGEM®-T Easy (Promega, UK), the resulting plasmid cut with BamHI and the *C. coli* *aphAIII* (*kan*) cassette (Wang and Taylor, 1990; van Vliet *et al.*, 1998) inserted. The resulting plasmid (pNC032) contained the kanamycin cassette in the same orientation as the interrupted *mfrX* gene. Plasmid pNC032 was introduced into *C. jejuni* NCTC11168 via electroporation and transformants selected as above. Potential *mfrX* mutants were confirmed by PCR using flanking primers *mfrX*-F and *mfrX*-R (Table S2).

Reverse transcriptase-PCR analysis

For analysis of *cj0411* expression in the *frdA* mutant and for the analysis of expression of *frdA* and *mfrA* in chemostat culture in response to anaerobiosis, the extraction of RNA, cDNA synthesis and qRT-PCR experiments followed the general methods previously described in Guccione and colleagues (2008). Culture samples were harvested directly into a mix of 62.5 μl prechilled phenol made up in 1.2 ml of 100% ethanol, to stabilize the RNA. Samples were then centrifuged (8000 g for 4 min, 4°C). Total RNA was purified from cell pellets using an RNeasy Mini kit (Qiagen, UK) as recommended by the suppliers. The RNA concentration and purity were determined using a Beckman DU 650 spectrophotometer. cDNA was synthesized using 4 μg of DNase treated RNA as described previously (Guccione *et al.*, 2008). Gene-specific primers (see supporting information in Table S2) were designed to amplify 50–150 nucleotide fragments of the target genes and the *gyrA* gene as an internal control, using PRIMER 3 software (Untergasser *et al.*, 2007). Reactions (15 μl) contained 7.5 μl Quantace sensimix buffer (Bioline, UK), 0.3 μl SYBR green solution (Bioline), 0.2 μM of each of the two primers for each gene and 3 μl cDNA in a MX3005P thermal cycler (Stratagene, UK). The thermal cycling conditions were as follows: 95°C for 10 min; 35 cycles of 95°C for 15 s, 61°C for 30 s. A standard curve was established for each gene studied using genomic DNA and the data analysed as previously described in Guccione and colleagues (2008), with target gene expression normalized to *gyrA* expression. No-template reactions were included as negative controls.

5' RACE

The transcription start site of the *mfr(X)ABE* operon was determined using 5' RACE as described previously (Wagner and Vogel, 2005). Briefly, 12 µg of RNA isolated from a mid log phase culture of *C. jejuni* NCTC 11168 using the RNeasy kit (Qiagen, UK) was treated with tobacco acid pyrophosphatase (TAP) and RNA oligonucleotide adaptor A3 (Table S2) was ligated to the 5' end of the treated RNA. TAP cleaves the 5'-triphosphate of primary transcripts to a monophosphate, thus making them available for ligation of the RNA adaptor. This results in an enrichment of 5'-RACE products for primary transcripts in TAP-treated RNA, in comparison with an untreated control. First strand cDNA synthesis was performed using gene-specific primers [mfrX5'RACE1 or mfrA5'RACE1 (Table S2)] followed by PCR amplification with nested gene-specific primers [mfrX5'RACE2 or mfrA5'RACE2 (Table S2)] and 5'-Adaptor-specific DNA primer B6. (Table S2). The resulting PCR products were cloned into the pGEM-T_{easy} cloning vector (Promega, UK) and the nucleotide sequence of the inserts was determined using standard protocols.

Succinate-dependent oxygen uptake rates

Succinate oxidation was determined by measuring the change in dissolved oxygen concentration of cell suspensions in a Clark-type oxygen electrode, linked to a chart recorder and calibrated using air saturated 25 mM phosphate buffer (pH 7.5) (219 nmol dissolved O₂ ml⁻¹ at 37°C). Cells were grown under microaerobic conditions in 200 ml BHI-FCS or MH overnight, and harvested by centrifugation at 10 000 g for 15 min at 4°C. The pellet obtained was then resuspended in 25 mM phosphate buffer (pH 7.5). A zero oxygen baseline was determined by the addition of sodium dithionite. The cell suspension was maintained at 37°C and stirred at a constant rate. Sodium succinate was added to a final concentration of 5 mM, by injection through a fine central pore in the airtight plug. Rates were expressed as nmol O₂ utilized min⁻¹ mg protein⁻¹.

Enzyme assays

All assays were performed at 37°C using a Shimadzu UV-2401PC spectrophotometer.

The 2,6-dichlorophenolindophenol (DCPIP) linked succinate dehydrogenase assays were performed aerobically in a 1 ml reaction mixture containing 20 mM potassium phosphate buffer pH 7.2, 2 mM KCN, 0.01 mM DCPIP, 4 mM phenazine methosulfate and an appropriate volume of *C. jejuni* cell-free extract. The reaction was started with 1 mM sodium succinate and the reduction of the DCPIP dye was followed at 600 nm. Any endogenous background rate was determined before the addition of succinate. Specific activities were calculated using an extinction coefficient for DCPIP of 21 mM⁻¹ cm⁻¹ at 600 nm. Benzyl viologen-linked fumarate reductase assays were carried out with intact cells or periplasmic extracts (see below) in a 1 ml assay mixture contained in a screw top glass cuvette with a silicone seal. All buffers and solutions were made anaerobic by sparging with

oxygen-free nitrogen. The final assay mixture contained 25 mM sodium phosphate buffer pH 7, 1 mM benzyl viologen and 5 mM sodium fumarate. After addition of cells or extract to the sparged buffer plus viologen mixture alone, aliquots of freshly prepared sodium dithionite solution were injected into the cuvette until a steady absorbance at 578 nm was achieved. The assay was initiated by the injection of an anaerobic solution of sodium fumarate. Activities with the fumarate analogues mesaconate and crotonate were measured using the same assay. Specific activities for all substrates were calculated using an extinction coefficient for benzyl viologen of 8.6 mM⁻¹ cm⁻¹ at 578 nm.

¹H nuclear magnetic resonance spectroscopy

Samples (1 ml) from cell suspensions incubated with 5 mM fumarate or mesaconate were centrifuged to remove cells (13 800 g, 5 min) and the supernatants used directly for nuclear magnetic resonance (NMR) analysis. ¹H-NMR was carried out using a Bruker DRX500 spectrometer operating at 500 MHz, as described by Leon-Kempis and colleagues (2006). Spectra were acquired into 4096 complex points over a spectral width of 12.5 kHz and the solvent (H₂O) signal reduced by presaturation for 2 s. Samples (0.45 ml supernatant plus 0.05 ml of D₂O) were run in 5-mm-i.d. diameter tubes at 25°C. Chemical shifts and concentrations were established by reference to 1 mM trimethylsilylpropionate (TSP; 0 p.p.m) added to all samples. For quantification of peak area, integration was performed using FELIX (Accelrys, San Diego, CA), and the following signals were used: fumarate, 6.49–6.55 p.p.m.; succinate, 2.35–2.45 p.p.m.; 2-methylfumarate (mesaconate) 1.86–1.96 p.p.m.; 2-methylsuccinate 1.06–1.13 p.p.m.

Preparation of periplasmic extracts

For 2D-gel proteomic analysis, the osmotic shock method of Myers and Kelly (2005) was used. Cells were grown microaerobically at 37°C in 200 ml BHI-FCS broth overnight. The cell suspension was centrifuged (15 000 g, 20 min at 4°C) and the resulting pellet was resuspended in 10 ml of 20% (w/v) sucrose, 30 mM Tris-HCl pH 8 at room temperature. EDTA was added to a final concentration of 1 mM and the suspension was poured into a 100 ml conical flask and stirred at 180 r.p.m. in a 25°C constant temperature room for 10 min. The suspension was then centrifuged (10 000 g, 10 min at 4°C) and the pellet was resuspended in ice-cold 10 mM Tris-HCl pH 8 to a volume of 10 ml and stirred at 180 r.p.m. in a 4°C constant temperature room for 10 min. The suspension was then centrifuged again (18 000 g, 15 min at 4°C) and the supernatant collected as the periplasmic fraction. For detection of periplasmic fumarate reductase activity and Western blotting, *C. jejuni* periplasm was isolated by the more rapid polymyxin-B treatment of whole cells, as described previously (Sommerlad and Hendrixson, 2007; Atack *et al.*, 2008). Contamination of the periplasm by cytoplasmic proteins was assayed using cytochrome *c* content as the periplasmic marker and isocitrate dehydrogenase (ICDH) activity as the cytoplasmic marker, using the assays described by Myers and Kelly

(2005). These assays showed that with both methods the cytoplasmic fraction routinely contained < 5% of the total cytochrome *c* content, while the periplasm contained < 10% of the total ICDH activity.

SDS-PAGE and immunoblotting

Proteins were separated by SDS-PAGE using the Mini-PROTEAN 3 apparatus (BIO-RAD, California, USA) on 10% (w/v) acrylamide gels. Transfer of proteins was carried out using a Mini Trans-Blot Cell (BIO-RAD). The gel-blot sandwich was constructed according to manufacturer's instructions and the proteins transferred to a nitrocellulose membrane (Hybond-C Extra, Amersham Biosciences) at a constant voltage of 100 V for 90 min at 4°C. All immunodetection steps were carried out at room temperature with constant agitation. TBS-T (25 mM Tris-HCl pH 7.4, 130 mM NaCl, 0.1% Tween 20) was used as both a base for blocking agent (5% dried skimmed-milk powder dissolved in TBS-T) and for washing. Primary polyclonal antibodies to MfrA were raised in rats from protein purified as above, and produced by Dr Simon Smith, BioServ UK, University of Sheffield. Crude serum was diluted in blocking agent (1:2000) and applied to the membrane. Membranes were reacted for approximately 1 h and washed in TBS-T before the secondary antibody (peroxidase-linked Anti-Rat IgG, Sigma UK) was diluted (1:2000) and applied to the membrane. Antibody binding was visualized by means of enhanced chemi-luminescence (ECL Kit, GE Healthcare, UK), according to manufacturer's instructions.

2D-gel electrophoresis and proteomics

Methods for the analysis of *C. jejuni* proteins on 2D-gels closely followed those described in Holmes and colleagues (2005) and Leon-Kempis and colleagues (2006). For the first dimension, 200 µg total sample protein was mixed with IPG rehydration buffer (7 M urea, 2 M thiourea, 2% CHAPS, 18 mM dithiothreitol (DTT), bromophenol blue and 2% pH 3-10 NL non-linear IPG buffer; final volume 370 µl) before loading onto 18 cm pH 3-10 NL Immobiline DryStrips (Amersham Biosciences, UK). Following overnight rehydration, IEF was performed for 80 kVh at 20°C over 24 h using the pHaser system (Genomic Solutions, UK). The focussed strips were treated as described previously (Leon-Kempis *et al.*, 2006). Second dimension 10% duracryl gels (28 × 23 cm, 1 mm thick) were prepared for use in the Investigator 2nd Dimension Running System (Genomic Solutions, UK), with electrophoresis at 500 V or 20 W per gel. Proteins were stained by Sypro-Ruby (Bio-Rad, UK) and the gels imaged using the Pharos FX+ Molecular Imager with Quantity One imaging software (Bio-Rad, UK). Protein spots were excised from the gel using the ProPick excision robot (Genomic Solutions, UK) and in-gel tryptic digestion performed as described by Holmes and colleagues (2005). Tryptic digests were analysed using a Reflex III MALDI-TOF instrument (Bruker, UK). Proteins were identified by the Protein Mass Fingerprint technique using the MASCOT search tool (Matrix Science; <http://matrixscience.com>).

Acknowledgements

This work was supported by grant BB/D008395/1 to DJK for SJH, and CASE studentships to EJG and AH from the UK Biotechnology and Biological Sciences Research Council (BBSRC) in partnership with Don Whitley Scientific Ltd (Shipley, UK). The Core Strategic Grant from the BBSRC supported the work at the IFR; Mass Spectroscopy was performed by Mike Naldrett at the Joint IFR/JIC Proteomic Facility. We also thank Dr S.E. Sedelnikova for assistance with protein purification and Dr Wendy Trotter for help with NMR.

References

- Atack, J.M., Harvey, P., Jones, M.A., and Kelly, D.J. (2008) The *Campylobacter jejuni* thiol peroxidases Tpx and Bcp both contribute to aerotolerance and peroxide-mediated stress resistance but have distinct substrate specificities. *J Bacteriol* **190**: 5279–5290.
- Bader, J., Gunther, H., Schleicher, E., Simon, H., Pohl, S., and Mannheim, W. (1980) Utilization of (E)-2-butenoate (crotonate) by *Clostridium kluveri* and some other *Clostridium* species. *Arch Microbiol* **125**: 159–165.
- Berks, B.C., Sargent, F., and Palmer, T. (2005) Protein targeting by the bacterial twin-arginine (Tat) pathway. *Curr Opin Microbiol* **8**: 174–181.
- Buckel, W. (2001) Unusual enzymes involved in five pathways of glutamate fermentation. *Appl Microbiol Biotechnol* **57**: 263–273.
- Butler, J.E., Glaven, R.H., Esteve-Nunez, A., Nunez, C., Shebololina, E.S., Bond, D.R., and Lovley, D.R. (2006) Genetic characterization of a single bifunctional enzyme for fumarate reduction and succinate oxidation in *Geobacter sulfurreducens* and engineering of fumarate reduction in *Geobacter metallireducens*. *J Bacteriol* **188**: 450–455.
- Carlone, G.M., and Anet, F.A.L. (1986) detection of menaquinone-6 and a novel methyl-substituted menaquinone-6 in *Campylobacter jejuni* and *Campylobacter fetus* subsp. *fetus*. *J Gen Microbiol* **129**: 3385–3393.
- Cecchini, G., Schroder, I., Gunsalus, R.P., and Maklashina, E. (2002) Succinate dehydrogenase and fumarate reductase from *Escherichia coli*. *Biochim Biophys Acta* **1553**: 140–157.
- Guccione, E.J., Leon-Kempis, M.D.R., Pearson, B.M., Hitchin, E., Mulholland, F., Van Diemen, P., *et al.* (2008) Amino-acid dependent growth of *Campylobacter jejuni*: Key roles for aspartase (AspA) under microaerobic and oxygen-limited conditions and identification of AspB (Cj0762), essential for growth on glutamate. *Mol Microbiol* **69**: 77–93.
- Gundogdu, O., Bentley, S.D., Holden, M.T., Parkhill, J., Dorrell, N., and Wren, B.W. (2007) Re-annotation and re-analysis of the *Campylobacter jejuni* NCTC11168 genome sequence. *BMC Genomics* **8**: 162.
- Hederstedt, L. (2002) Succinate: quinone oxidoreductase in the bacteria *Paracoccus denitrificans* and *Bacillus subtilis*. *Biochim Biophys Acta* **1553**: 74–83.
- Hemm, M.R., Paul, B.J., Schneider, T.D., Storz, G., and Rudd, K.E. (2008) Small membrane proteins found by comparative genomics and ribosome binding site models. *Mol Microbiol* **70**: 1487–1501.

- Holmes, K., Mulholland, F., Pearson, B.M., Pin, C., McNicholl-Kennedy, J., Ketley, J.M., and Wells, J.M. (2005) *Campylobacter jejuni* gene expression in response to iron limitation and the role of Fur. *Microbiology* **151**: 243–257.
- Jacobs-Reitsma, W., Lyths, U., and Wagenaar, J. (2008) *Campylobacter* in the food supply. In *Campylobacter*, 3rd edn. Nachamkin, I., Szymanski, C.M., and Blaser, M.J. (eds). Washington, DC, USA: ASM Press, pp. 627–644.
- Janssen, S., Schäfer, G., Anemüller, S., and Moll, R. (1997) A succinate dehydrogenase with novel structure and properties from the hyperthermophilic archaeon *Sulfolobus acidocaldarius*: genetic and biophysical characterisation. *J Bacteriol* **179**: 5560–5569.
- Juhnke, H.D., Hiltcher, H., Nasiri, H.R., Schwalbe, H., and Lancaster, C.R. (2009) Production, characterization and determination of the real catalytic properties of the putative 'succinate dehydrogenase' from *Wolinella succinogenes*. *Mol Microbiol* **71**: 1088–1101.
- Karlyshev, A.V., and Wren, B.W. (2005) Development and application of an insertional system for gene delivery and expression in *Campylobacter jejuni*. *Appl Environ Microbiol* **71**: 4004–4013.
- Kelly, D.J. (2008) Complexity and versatility in the physiology and metabolism of *Campylobacter jejuni*. In *Campylobacter*, 3rd edn. Nachamkin, I., Szymanski, C.M., and Blaser, M.J. (eds). Washington, DC, USA: ASM Press, pp. 41–61.
- Lancaster, C.R. (2002) Succinate: quinone oxidoreductases: an overview. *Biochim Biophys Acta* **1553**: 1–6.
- Lancaster, C.R., Sauer, U.S., Gross, R., Haas, A.H., Graf, J., Schwalbe, H., et al. (2005) Experimental support for the 'E pathway hypothesis' of coupled transmembrane e⁻ and H⁺ transfer in dihemic quinol: fumarate reductase. *Proc Natl Acad Sci USA* **102**: 18860–18865.
- Lancaster, C.R., and Simon, J. (2002) Succinate: quinone oxidoreductases from epsilon-proteobacteria. *Biochim Biophys Acta* **1553**: 84–101.
- Lemos, R.S., Gomes, C.M., and Teixeira, M. (2001) *Acidianus ambivalens* Complex II typifies a novel family of succinate dehydrogenases. *Biochem Biophys Res Commun* **281**: 141–150.
- Lemos, R.S., Fernandes, A.S., Pereira, M.M., Gomes, C.M., and Teixeira, M. (2002) Quinol: fumarate oxidoreductases and succinate: quinone oxidoreductases: phylogenetic relationships, metal centres and membrane attachment. *Biochim Biophys Acta* **1553**: 158–170.
- Leon-Kempis, M.D.R., Guccione, E., Mulholland, F., Williamson, M.P., and Kelly, D.J. (2006) The *Campylobacter jejuni* PEB1a adhesin is an aspartate/glutamate-binding protein of an ABC transporter essential for microaerobic growth on dicarboxylic amino acids. *Mol Microbiol* **60**: 1262–1275.
- Mileni, M., Macmillan, F., Tziatzios, C., Zwicker, K., Haas, A.H., Mantele, W., et al. (2006) Heterologous production in *Wolinella succinogenes* and characterisation of the quinol: fumarate reductase enzymes from *Helicobacter pylori* and *Campylobacter jejuni*. *Biochem J* **395**: 191–201.
- Myers, J.D., and Kelly, D.J. (2005) A sulphite respiration system in the chemoheterotrophic human pathogen *Campylobacter jejuni*. *Microbiology* **151**: 233–242.
- Pajaniappan, M., Hall, J.E., Cawthraw, S.A., Newell, D.G., Gaynor, E.C., Fields, J.A., et al. (2008) A temperature-regulated *Campylobacter jejuni* gluconate dehydrogenase is involved in respiration-dependent energy conservation and chicken colonization. *Mol Microbiol* **68**: 474–491.
- Parkhill, J., Wren, B.W., Mungall, K., Ketley, J.M., Churcher, C., Basham, D., et al. (2000) The genome sequence of the food-borne pathogen *Campylobacter jejuni* reveals hyper-variable sequences. *Nature* **403**: 665–668.
- Petersen, L., Larsen, T.S., Ussery, D.W., On, S.L., and Krogh, A. (2003) RpoD promoters in *Campylobacter jejuni* exhibit a strong periodic signal instead of a -35 box. *J Mol Biol* **326**: 1361–1372.
- Pittman, M.S., Elvers, K.T., Lee, L., Jones, M.A., Poole, R.K., Park, S.F., and Kelly, D.J. (2007) Growth of *Campylobacter jejuni* on nitrate and nitrite: electron transport to NapA and NrfA via NrfH and distinct roles for NrfA and the globin Cgb in protection against nitrosative stress. *Mol Microbiol* **63**: 575–590.
- Sambrook, J., Fritsch, E.F., and Maniatis, T. (1989) *Molecular Cloning: a Laboratory Manual*, 2nd edn. Cold Spring Harbour, NY, USA: Cold Spring Harbour Laboratory Press.
- Sellars, M.J., Hall, S.J., and Kelly, D.J. (2002) Growth of *Campylobacter jejuni* supported by respiration of fumarate, nitrate, nitrite trimethylamine-N-Oxide, or dimethyl sulfoxide requires oxygen. *J Bacteriol* **184**: 4187–4196.
- Sommerlad, S.M., and Hendrixson, D.R. (2007) Analysis of the Roles of FlgP and FlgQ in Flagellar Motility of *Campylobacter jejuni*. *J Bacteriol* **189**: 179–186.
- Thauer, R.K., Jungermann, K., and Decker, K. (1977) Energy conservation in chemotrophic anaerobic bacteria. *Bacteriol Rev* **41**: 100–180.
- Untergasser, A., Nijveen, H., Rao, X., Bisseling, T., Geurts, R., and Leunissen, J.A. (2007) Primer3Plus, an enhanced web interface to Primer3. *Nucleic Acids Res* **35** (Web Server issue): W71–74.
- van Vliet, A.H.M., Wooldridge, K.G., and Ketley, J.M. (1998) Iron-responsive gene regulation in a *Campylobacter jejuni* mutant. *J Bacteriol* **180**: 5291–5298.
- Wagenaar, J.A., Jacobs-Reitsma, W., Hofshagen, M., and Newell, D. (2008) Poultry colonisation with *Campylobacter* and its control at the primary production level. In *Campylobacter*, 3rd edn. Nachamkin, I., Szymanski, C.M., and Blaser, M.J. (eds). Washington, DC, USA: ASM Press, pp. 667–678.
- Wagner, E.G.H., and Vogel, J. (2005) Approaches to Identify Novel Non-messenger RNAs in Bacteria and to Investigate their Biological Functions: Functional Analysis of Identified Non-mRNAs. In *Handbook of RNA Biochemistry*, Vol. 2. Hartmann, R.K., Bindereif, A., Schön, A., and Westhof, E. (eds). Weinheim, Germany: Wiley-VCH Verlag GmbH & Co. KGaA, pp. 614–642.
- Wang, Y., and Taylor, D.E. (1990) Chloramphenicol resistance in *Campylobacter coli*: nucleotide sequence, expression, and cloning vector construction. *Gene* **94**: 23–28.
- Weerakoon, D.R., Borden, N.J., Goodson, C.M., Grimes, J., and Olson, J.W. (2009) The role of respiratory donor enzymes in *Campylobacter jejuni* host colonization and physiology. *Microb Pathog* **47**: 8–15.
- Weingarten, R.A., Grimes, J.L., and Olson, J.W. (2008) The role of *Campylobacter jejuni* respiratory oxidases and

- reductases in host colonization. *Appl Environ Microbiol* **74**: 1367–1375.
- Weingarten, R.A., Taveirne, M.E., and Olson, J.W. (2009) The dual functioning fumarate reductase is the sole succinate : quinone reductase in *Campylobacter jejuni* and is required for full host colonisation. *J Bacteriol* **191**: 5293–5300.
- Woodall, C.A., Jones, M.A., Barrow, P.A., Hinds, J., Marsden, G.L., Kelly, D.J., et al. (2005) *Campylobacter jejuni* gene expression in the chick cecum: evidence for adaptation to a low-oxygen environment. *Infect Immun* **73**: 5278–5285.
- Zaunmüller, T., Kelly, D.J., Glockner, F.O., and Uden, G. (2006) Succinate dehydrogenase functioning by a reverse redox loop mechanism and fumarate reductase in sulphate-reducing bacteria. *Microbiology* **152**: 2443–2453.

Supporting information

Additional Supporting Information may be found in the online version of this article:

Table S1. Defined media for growth of *C. jejuni* in chemostat culture.

Table S2. Primers used in this study.

Please note: Wiley-Blackwell are not responsible for the content or functionality of any supporting materials supplied by the authors. Any queries (other than missing material) should be directed to the Correspondence for the article.